



2950 Niles Road, St. Joseph, MI 49085-9659, USA
269.429.0300 fax 269.429.3852 hq@asabe.org www.asabe.org

An ASABE Meeting Presentation

DOI: 10.13031/aim.20152181312

Paper Number: 152181312

Spectral band selection to design a low cost sensor for citrus black spot disease detection

Alireza Pourreza, Postdoctoral Research Associate

Department of Agricultural and Biological Engineering, University of Florida, Gainesville FL 32611,
apourreza@ufl.edu

Won Suk Lee, Professor

Department of Agricultural and Biological Engineering, University of Florida, Gainesville FL 32611,
wslee@ufl.edu

Rebekah Combs, Undergraduate Student

Department of Agricultural and Biological Engineering, University of Florida, Gainesville FL 32611,
recombs@ufl.edu

Pamela Roberts, Professor

Department of Plant Pathology, University of Florida, Immokalee, FL 34142, pdr@ufl.edu

Mark Ritenour, Associate Professor

Department of Horticultural Sciences, University of Florida, Fort Pierce, FL 34845, ritenour@ufl.edu

Written for presentation at the

2015 ASABE Annual International Meeting

Sponsored by ASABE

New Orleans, Louisiana

July 26 – 29, 2015

Abstract. *Guignardia citricarpa* Kiely (Anamorph: *Phyllosticta citricarpa* (McAlpine) Van der Aa) or citrus black spot (CBS) is a citrus fungal disease found in 2010 in south Florida that causes premature fruit drop and yield loss particularly on late harvested varieties such as Valencia. CBS symptoms on citrus fruit occur in various forms; however, hard spot and cracked spot are the most common symptoms. In this study, spectral characteristic of several CBS symptoms were investigated to determine the best spectral bands for diagnosis. Color images of CBS symptoms as well as healthy fruits were acquired using a digital single-lens reflex camera. Band selection was conducted with respect to spectral response of the camera. A set of color features were extracted from red, green, and blue channels of the color images for classification. A classification model was developed using various classifiers and k-fold cross validation which was able to accurately detect the CBS symptoms along with the level of

The authors are solely responsible for the content of this meeting presentation. The presentation does not necessarily reflect the official position of the American Society of Agricultural and Biological Engineers (ASABE), and its printing and distribution does not constitute an endorsement of views which may be expressed. Meeting presentations are not subject to the formal peer review process by ASABE editorial committees; therefore, they are not to be presented as refereed publications. Citation of this work should state that it is from an ASABE meeting paper. EXAMPLE: Author's Last Name, Initials. 2015. Title of Presentation. ASABE Paper No. ---. St. Joseph, Mich.: ASABE. For information about securing permission to reprint or reproduce a meeting presentation, please contact ASABE at rutter@asabe.org or 269-932-7004 (2950 Niles Road, St. Joseph, MI 49085-9659 USA).

severity. The results showed that the spectral analysis could provide useful information to develop an efficient color image classification algorithm for CBS detection. CBS-positive spots were classified with a 100% accuracy using this algorithm. CBS lesion type and the maturity of healthy fruits were also identified with accuracies of 69% and 98%, respectively.

Keywords. Black spot, citrus, disease, machine vision, spectral analysis

Introduction

In March of 2010, citrus black spot (CBS) was first detected on 'Valencia' sweet oranges in Florida near the Immokalee area. This was the first development in North America and quite a distance from the nearest known infestations in Argentina and Brazil (Schubert, Sutton, & Jeyaprakash, 2010). Two months later CBS was discovered 14 miles northeast of the first location (Dewdney, Peres, Ritenour, & Roberts, 2015). Currently Collier, Hendry, Lee and Polk counties are quarantined for containing the disease (El-Lissy, 2015). Citrus black spot is a fungal disease caused by *Guignardia citricarpa* Kiely (Anamorph: *Phyllosticta citricarpa* (McAlpine) Van der Aa) that produces lesions on citrus fruit as well as hybrids. While the outside rind is damaged, the inside of the fruit is not effected; however, the fruit value for selling as fresh produce is reduced. This disease can also cause premature fruit drop (Dewdney & Peres, 2010). Immature fruit drop is a critical concern in Florida because it seriously affects crop yield (Choi, Lee, Ehsani, & Roka, 2015). Air currents can carry the wind-borne ascospores ejected from infected leaves in the leaf litter under trees. The pathogen can also be spread by rain splashing on infected fruit and/or leaf litter, but this only causes the spores to move a short distance. Long distance travel can be achieved during the latent phase (infection is not visible) when infected leaf debris or nursery stock is transported (Dewdney et al., 2015).

CBS expresses various fruit symptoms which can make it difficult to distinguish the disease. Hard spot is the most characteristic of the disease and looks like a small round sunken lesion with a red-brown margin and tan center. False melanose is a large quantity of small, slightly raised lesions with a smooth texture. Cracked spot is consisted of large, flat, dark brown lesions with raised cracks in the surface. Virulent spot is the combination or fusion of several lesions and can cover a significant portion of the fruit surface (Dewdney & Peres, 2010). A combination of these symptoms can make detection even more difficult.

There are currently two techniques for detecting CBS: Polymerase Chain Reaction (PCR) and hyperspectral imaging. PCR amplifies a DNA sequence of the fungus by making millions of copies of a specific section of the DNA in order to provide enough material to detect. Synthetic primers are required to start the process of DNA production. At the University of Pretoria, a set of primers was discovered to consistently diagnose *Guignardia citricarpa* within one day. This test was developed to distinguish between the regulated *Guignardia citricarpa* and the harmless endophyte *Guignardia mangiferae*. While the test was accurate on hard spot lesions, the procedure was not as accurate with the presence of false melanose and/or freckle spot (Meyer, Sanders, Jacobs, & Korsten, 2006). The second method of detection, hyperspectral imaging, combines images taken at a range of wavebands into one cube matrix. The hyperspectral image contains reflectance data from each band which results in a large amount of excess data. Bulanon, Burks, Kim, and Ritenour (2013) used hyperspectral imaging to identify CBS. Through testing, they discovered four bands that could be used to identify CBS: 493 nm, 629 nm, 713 nm, and 781 nm. Using artificial neural networks (ANN) and linear discriminant classifier (LDC) they detected CBS and market ready citrus with a 100% accuracy. With the addition of melanose, windscar and greasy spot, the accuracy dropped as low as 73.3%. This led to an overall accuracy of 92% for both classifiers. The overall accuracy was increased to 96.7% by combining the 713 nm and 781 nm wavelengths by using the Normalized Difference Vegetation Index (NDVI). In a different study, CBS classification was increased to 97.9% using the spectral angle mapper (SAM) approach with an optimal threshold value of 0.09 and 97.14% using the spectral information divergence (SID) mapping with a 0.04 optimal threshold (Kim, Burks, Ritenour, & Qin, 2014).

Spectroscopy, also known as spectral analysis, has been used to identify diseases in citrus. Spectral analysis studies a material's interaction with electromagnetic energy in order to determine the material's spectral properties. The signals given off by the compounds allow for the detection of substances within an object. Visible-near infrared spectroscopy (NIR) (Sankaran, Mishra, Maja, & Ehsani, 2011) and mid-infrared spectroscopy (Sankaran, Ehsani, & Etxeberria, 2010) have been used to detect Huanglongbing (HLB) in citrus. Citrus canker (Qin, Burks, Ritenour, & Bonn, 2009) as well as citrus variegated chlorosis (CVC) (Cardinali et al., 2012) have also been diagnosed with the use of spectroscopy.

The main objective of this study was to develop an image analysis algorithm for CBS diagnosis using the spectral characteristics of CBS symptoms. The specific objectives were: (1) to determine the spectral characteristics of several CBS symptoms; (2) to develop an image analysis algorithm for CBS diagnosis; and (3) to assess the classification accuracy using the proposed algorithm.

Materials and Methods

Data Collection

In April of 2015, a total of 135 Valencia citrus fruit (105 CBS-positive and 30 CBS-negative) were collected from a grove near Immokalee, Florida. Up to five spots on each sample were randomly marked for further image acquisition and spectral reflectance measurement. CBS-positive spots were categorized into five types of lesions including early hard spot, advance hard spot, cracked spot, early virulent spot, and virulent spot. CBS-negative samples were also categorized into two subclasses: healthy mature fruit, and healthy immature green fruit.

Spectral Reflectance Measurement

The spectral reflectance of the target spots were measured with a portable spectrometer (USB2000+, Ocean Optics, Inc., Dunedin, Florida) with a spectral resolution of ~0.3 nm. The spectrometer was capable of recording a spectral reflectance between 340 nm to 1030 nm. A fiber optic reflection probe (QR600-7-SR-125F, Ocean Optics, Inc., Dunedin, Florida) with a core diameter of 600 μm was used in conjunction with the portable spectrometer to measure spectral reflectance. In order to keep the probe positioned at a constant 45° to the target spots in all measurements, a reflection probe holder (RPH-1, Ocean Optics, Inc., Dunedin, Florida) was used. A certified reflectance standard (SRS-99-020, Labsphere, Inc., North Sutton, New Hampshire) was used to collect the optical reference standard before each measurement. To prevent additional noise in the spectral measurements, a light source (LS-1, Tungsten Halogen Light Source, Ocean Optics, Inc., Dunedin, Florida) of the spectrometer was turned on 45 minutes before measurement. The measurement was taken on April 2, 2015.

Spectral Measurement Error

Three different reference standards with a reflectance of 99%, 75%, and 50% each, were used to provide the optical reference standard. After waiting 45 minutes for the light source to warm up, reflectance measurements for each reference standard were taken every five minutes for an hour. This resulted in 12 reflectance measurements for each white standard. The means and standard deviations were then calculated to evaluate the spectrometer sensitivity and accuracy at different wavebands within the range of 340 nm to 1030 nm.

Image Acquisition

Color images of the fruit samples were acquired using a canon 5D Mark III (DS126321, Canon U.S.A. Inc., Lake Success, New York). A pair of fluorescent lights (SL Series Twin 13 watt IP65, StockerYale, Salem, New Hampshire) were placed at 45° for even illumination. All of the sample images were taken from the same distance and camera settings with an f stop of 1/5.6, exposure of 1/60 seconds and ISO speed of 100.

Color Feature Extraction

Features were extracted from normalized histograms of red, green, and blue channels of the color images to use in classification. These features included mean, standard deviation, third moment, smoothness, uniformity, entropy, maximum gray-level probability, and range (Pourreza, Lee, Raveh, Ehsani, & Etxeberria, 2014).

Bands/Features Ranking

The Scaled Alignment Selection (SAS) feature selection method was used for selecting both bands and color features (Ramona, Richard, & David, 2012). The measures of relevance of bands/features were normalized by the highest ranked band/feature. The normalized measures of relevance for wavelengths were plotted to visualize important bands. The best color features were also selected based on the best classification accuracy achieved with minimum number of top features.

Classification

Figure 1 illustrates the classification model for the dataset. The first step was identifying the possibility of the presence of CBS. If the test was positive, then second step determined the expressed symptom. If the test was negative, the third step classified the fruit as mature or immature healthy fruit. The samples were classified using five supervised learning methods including linear, naive Bayes linear, quadratic, naive Bayes quadratic, and Mahalanobis and were evaluated using MATLAB functions. A k-fold (10-fold) cross-validation method was adopted in all classification steps to affirm that the results were independent of the validation and training sets.

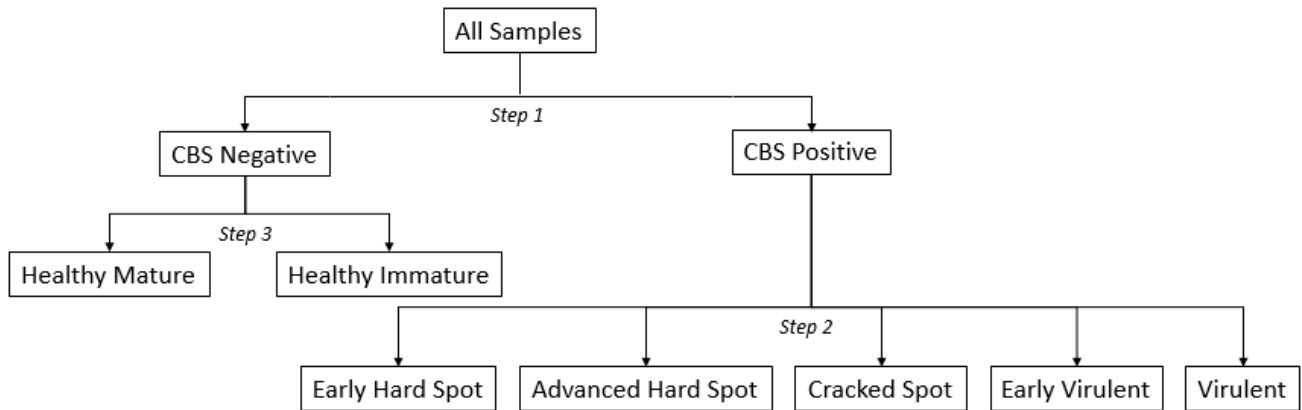


Figure 1. Classification model for CBS detection, CBS lesion type identification, and maturity recognition, at steps 1, 2, and 3, respectively.

Results and Discussion

Dataset Validation

A set of citrus fruit with various types of CBS symptoms was created. Several observations were conducted by a number of experts and two plant pathologists to determine and validate the CBS symptoms classes. The dataset included 140 early hard spots, 130 advanced hard spots, 32 cracked spots, 103 early virulent, and 82 virulent samples as the CBS subclasses as well as 86 mature, and 64 immature samples as the control subclasses.

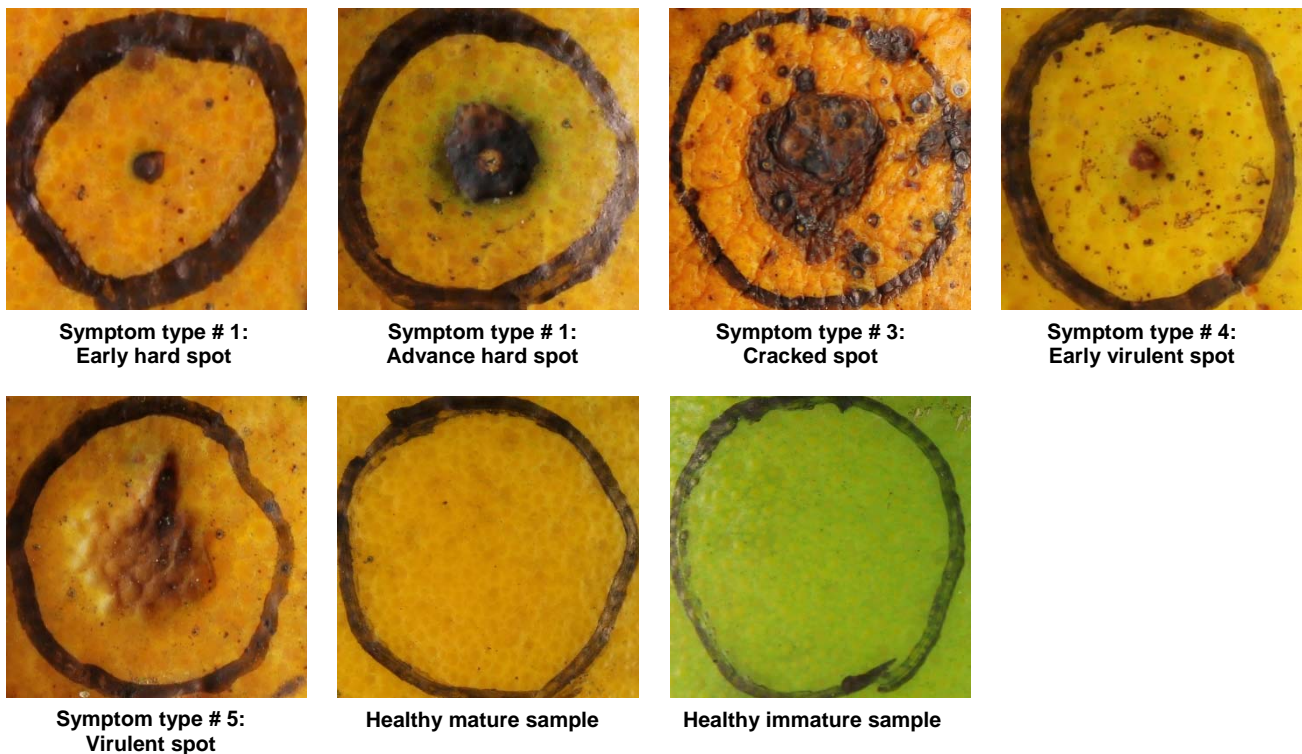


Figure 2. Color images of CBS-positive samples in five classes as well as two CBS-negative classes.

Spectral Measurement Error

All of the reflectance data for the reference standards, as well as their means, were combined and illustrated in Figure 3. It is clear the data results varied as time progressed. Data located outside the 350 nm – 900 nm range represents the ultraviolet and infrared ranges which fall outside of the spectroscopy sensitivity range. Further observation at the 99%, 75% and 50% standard reflectance revealed there was no correlation between time

(after the spectrometer was calibrated) and measured reflectance.

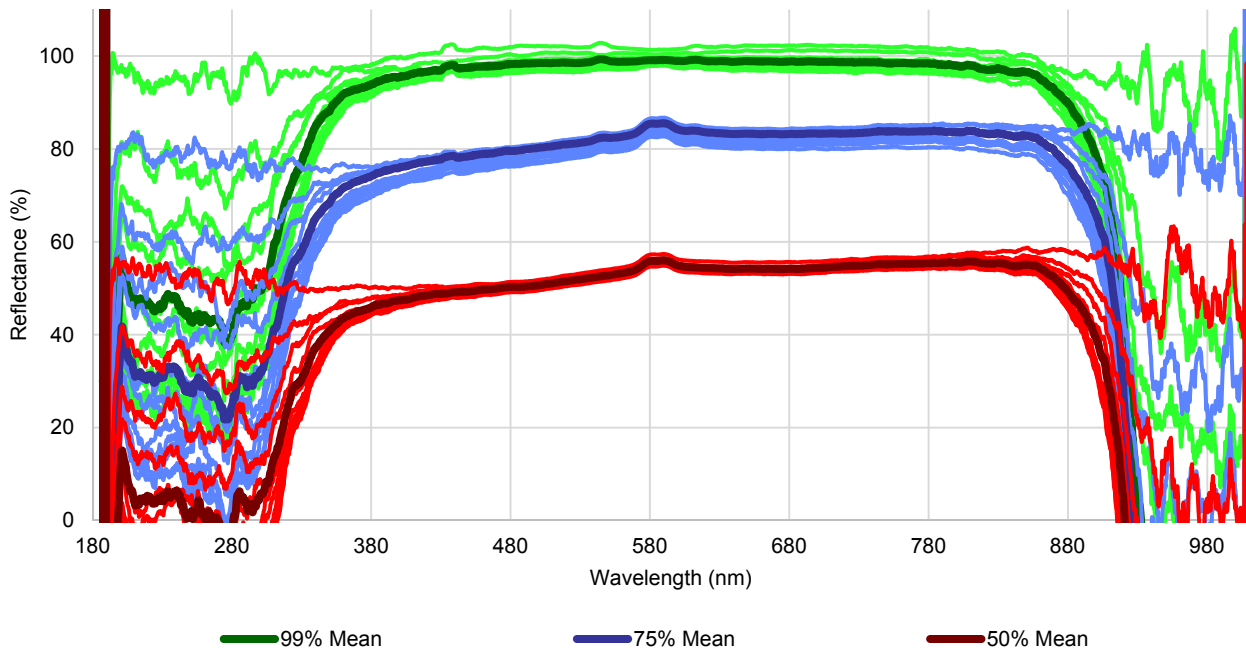


Figure 3. White standards reflectance measured over one hour along with the mean spectral reflectance for each white standard.

Figure 4 also shows the standard deviations of the spectral reflectance of three standards measured over one hour. The standard deviations below 350 nm and over 900 nm were increased compared to the deviation within 350-900 nm. These results showed that the spectrometer was accurate within 350-900 nm but it was not that sensitive beyond this range. Figure 4 also illustrates that the 50% white standard had the most consistent readings, while the 75% white standard had the least consistent readings.

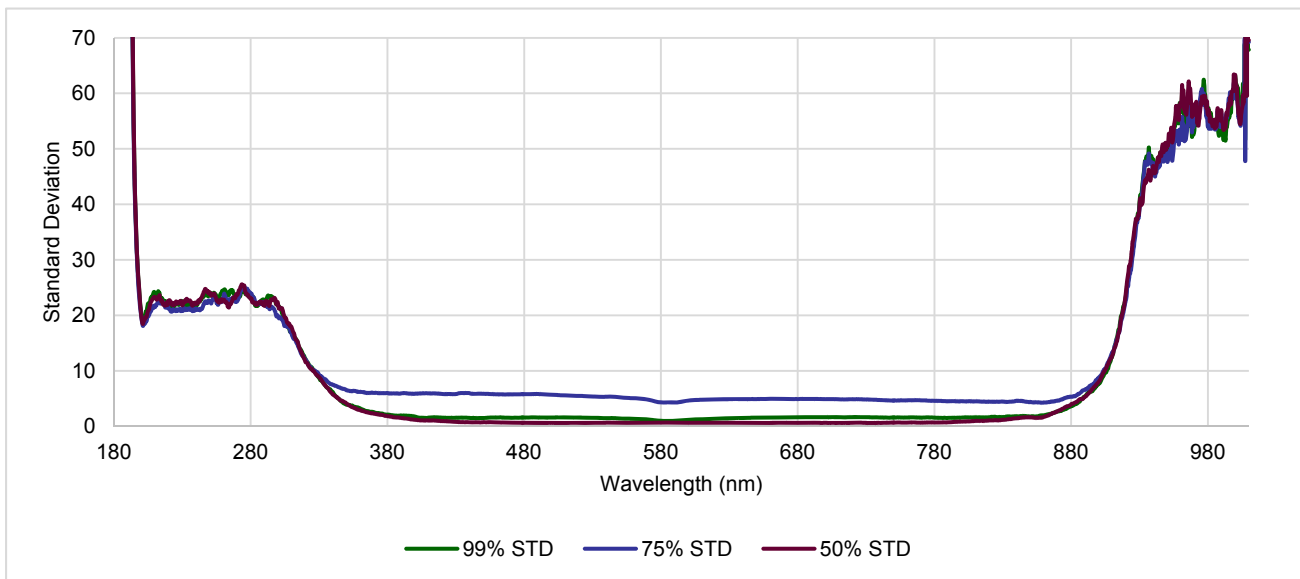


Figure 4. Standard deviation of standard reflectance measured over one hour.

Spectral Signatures

Figure 5 displays the average spectral reflectance of different CBS lesions and healthy samples as well as the sensitive bands of the three color channels in DSLR cameras. Generally, the CBS-positive classes absorbed more light within the visible region compared to the CBS-negative classes. Mature healthy fruits were clearly separable within the green and red channels; however, the spectral signatures of immature healthy fruits were relatively similar to early hard spot and early virulent within the red channel. In the CBS-positive class, advanced hard spots, cracked spots, and virulent spots had comparatively different signatures from the early hard spots

and early virulent spots within the green and red channels. This difference increased slightly in the NIR band between 700-850 nm.

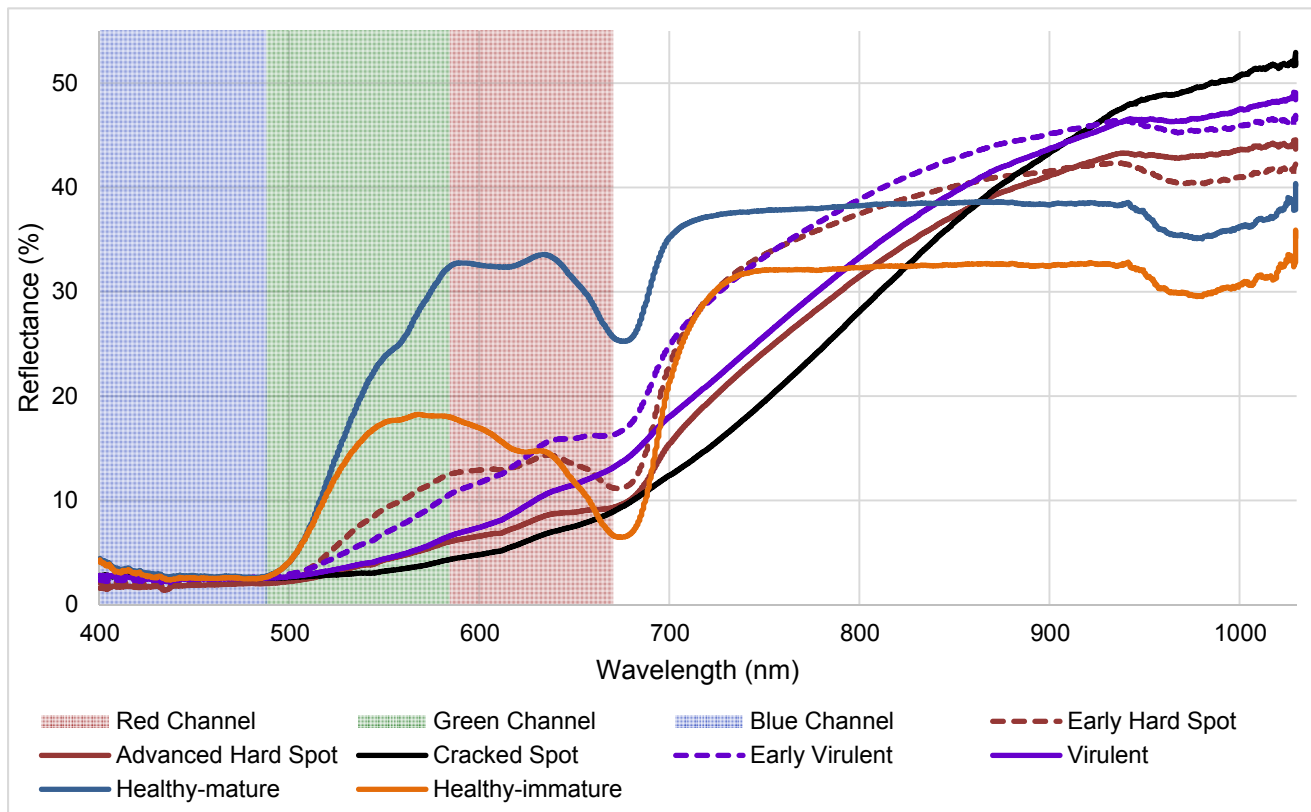


Figure 5. Mean spectral reflectance of the healthy and CBS spots as well as the sensitive bands for red, green, and blue channels of DSLR cameras.

Band Selection

The SAS procedure was conducted for spectral data and color features and for each step of the classification model, separately. Figure 6 displays the wavelengths with the most relevant information for classification in the three steps along with the sensitive bands of the three color channels in DSLR cameras.

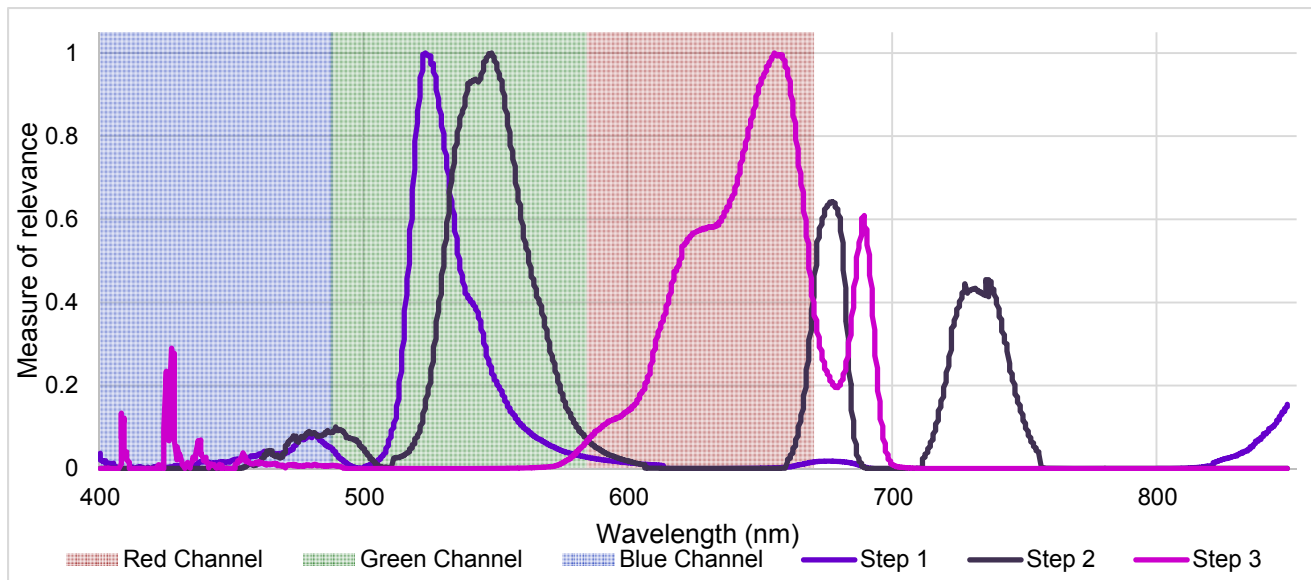


Figure 6. Normalized coefficient of the wavelength for each step within each color band.

At the step one of the classification model, all samples were classified into either CBS-positive or CBS-negative

super classes. Important wavelengths for the step one were mostly found within the green channel of the camera sensor at around 523 nm. As shown in figure 5, the spectral reflectance of CBS-negative classes centered around 523 nm. The variation within the CBS-positive subclasses was also relatively small at around this waveband. Significant wavelengths for step two of the classification model (identification of the CBS lesion types) were also in the green channel (549 nm) as well as in the red and NIR region (678 nm and 730 nm) and blue channel (480 nm) with smaller measure of relevance. The mature and immature CBS-negative subclasses were identified at the third step of the classification model and mostly in the red channel (655 nm, and 690 nm) as well as some wavelengths with smaller measure of relevance in the blue channel (427 nm).

Classification and Important Color Features

The confusion matrix including the classification rates and misclassification errors is shown in table 1. Figure 7 also illustrates the important color features for each step of the classification model. The CBS-negative/positive samples were identified with a 100% accuracy using the top three color features and a naïve Bayes quadratic classifier. The three features used at the step one included gray values mean, uniformity, and maximum gray-level probability, all extracted from the green channel of color images. This results strongly support the band selection outcomes in figure 6 that suggested the green channel contained the most important information for CBS identification. The types of CBS lesions were identified with an overall accuracy of 69% in the step two of the classification model using the top 14 color features (figure 7) and a linear classifier. The features used for CBS lesions identification included seven features from the green channel, five features from the blue channel, and two features from the red channel. Although the second important waveband (678 nm) for the step two is close to the red channel, the internal NIR cutoff filter in the DSLR camera limits the lights around this wavelength, and the red sensor in the camera does not receive much reflectance at 678 nm and beyond. That is why only two features from the red channel were identified important for the step two. Advanced hard spots were identified with the highest accuracy of 76.2%, while the virulent spots were detected with the lowest accuracy (52.4%). The virulent spots were mostly misclassified as early virulent or cracked spot. CBS negative samples were classified into mature and immature subclasses with a 98% accuracy using top six color features and a linear classifier. The top two features were extracted from red channel (figure 7) that supports the results of band selection for step three in figure 6. The other features were selected from green channel (two features) and red channel (two features). Out of 86 healthy-mature, 85 were identified correctly while only one was misclassified as healthy-immature. Out of 64 healthy-immature, 62 were identified correctly while only two were misclassified as healthy-mature.

Table 1. Number of samples classified/misclassified into each of the seven classes along with their corresponding classification rates and misclassification errors (%).

Prediction		Actual Class							Sum
		CBS Positive					CBS Negative		
		Early Hard Spot	Advanced Hard Spot	Cracked Spot	Early Virulent	Virulent	Healthy-mature	Healthy-immature	
CBS Positive	Early Hard Spot	104 (74.3%)	13 (10%)	0	13 (12.6%)	3 (3.7%)	0	0	133
	Advanced Hard Spot	14 (10%)	99 (76.2%)	6 (18.8%)	5 (4.9%)	7 (8.5%)	0	0	131
	Cracked Spot	1 (0.7%)	8 (6.2%)	24 (75%)	2 (1.9%)	17 (20.7%)	0	0	52
	Early Virulent	14 (10%)	0	0	66 (64.1%)	12 (14.6%)	0	0	92
	Virulent	7 (5%)	10 (7.7%)	2 (6.2%)	17 (16.5%)	43 (52.4%)	0	0	79
CBS Negative	Healthy-mature	0	0	0	0	0	85 (98.8%)	2 (3.1%)	87
	Healthy-immature	0	0	0	0	0	1 (1.2%)	62 (96.9%)	63
Sum		140	130	32	103	82	86	64	637

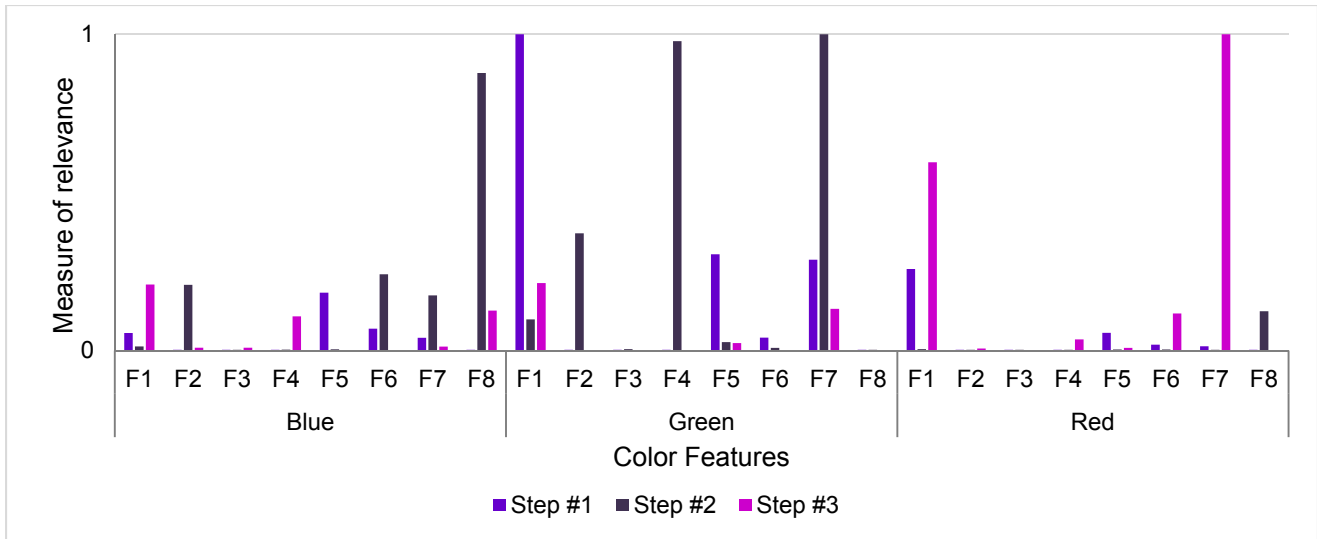


Figure 7. Normalized coefficient for each feature within each color band. The features from F1 to F8 are mean, standard deviation, third moment, smoothness, uniformity, entropy, maximum gray-level probability, and range.

Conclusion

The main objective of this study was to develop an image analysis algorithm for CBS diagnosis using the spectral characteristics of CBS symptoms. Spectral reflectance of various CBS-positive symptoms as well as mature and immature CBS-negative samples were measured and analyzed to determine the important wavebands for CBS diagnosis as well as lesion type identification. Then, the spectral band selection results were compared to the results of color feature selection to determine whether spectral analysis can justify the use of specific color information in an image classification algorithm and if it can help to develop a more efficient sensing system. The results showed that the features used in the classification model strongly support the band selection outcomes. For step one of the classification model, the most valuable information was found within the green band which resulted in an accuracy of 100% for CBS diagnosis. Two important wavebands for the step two were located in the near-infrared band which was beyond the range of most DSLR cameras. Since the camera employed in this study was unable to capture information in this range, therefore valuable information was lost. By removing the NIR cutoff filter from the camera, this information can be captured and used to produce a more accurate classification. For the step three of the model, helpful information was mainly found in the red band which resulted in an overall accuracy of 98% for CBS-negative maturity determination.

References

- Bulanon, Duke M, Burks, Thomas F, Kim, Dae G, & Ritenour, Mark A. (2013). Citrus black spot detection using hyperspectral image analysis. *Agricultural Engineering International: CIGR Journal*, 15(3), 171-180.
- Cardinali, Marcelo Camponez do Brasil, Boas, Paulino Ribeiro Villas, Milori, Débora Marcondes Bastos Pereira, Ferreira, Ednaldo José, e Silva, Marina França, Machado, Marcos Antonio, & Bellete, Barbara Sayuri. (2012). Infrared spectroscopy: A potential tool in huanglongbing and citrus variegated chlorosis diagnosis. *Talanta*, 91, 1-6.
- Choi, Daeun, Lee, Won Suk, Ehsani, Reza, & Roka, Fritz. (2015). A machine vision system for quantification of early fruit drop. *Transaction on ASABE*, 54(4), 933-946. doi: 10.13031/trans.58.10688
- Dewdney, Megan, & Peres, Natalia. (2010). Citrus Black Spot (*Guignardia citricarpa*): Identification, Biology and Control. Retrieved from UF/IFAS Citrus Extension website: http://irrec.ifas.ufl.edu/postharvest/pdfs/past_events/2010_presentations/Dewdney_Peris-CBS.pdf
- Dewdney, Megan, Peres, Natalia, Ritenour, Mark, & Roberts, Pamela. (2015). Citrus Extension Black Spot. from http://www.crec.ifas.ufl.edu/extension/black_spot/citrus_black_spot.shtml
- El-Lissy, Osama. (2015). *APHIS Expands Citrus Black Spot (Guignardia citricarpa) Regulated Area in South Florida* United States Department of Agriculture Retrieved from

http://www.aphis.usda.gov/plant_health/plant_pest_info/citrus/downloads/black_spot/DA-2015-16.pdf.

- Kim, Daegwan, Burks, Thomas F, Ritenour, Mark A, & Qin, Jianwei. (2014). Citrus black spot detection using hyperspectral imaging. *International Journal of Agricultural and Biological Engineering*, 7(6), 20-27.
- Meyer, L., Sanders, G. M., Jacobs, R., & Korsten, L. (2006). A One-Day Sensitive Method to Detect and Distinguish Between the Citrus Black Spot Pathogen *Guignardia citricarpa* and the Endophyte *Guignardia mangiferae*. *Plant Disease*, 90(1), 97-101. doi: 10.1094/PD-90-0097
- Pourreza, A, Lee, WS, Raveh, E, Ehsani, R, & Etxeberria, E. (2014). Citrus Huanglongbing detection using narrow-band imaging and polarized illumination. *Trans. ASABE*, 57(1), 259-272.
- Qin, Jianwei, Burks, Thomas F., Ritenour, Mark A., & Bonn, W. Gordon. (2009). Detection of citrus canker using hyperspectral reflectance imaging with spectral information divergence. *Journal of Food Engineering*, 93(2), 183-191. doi: <http://dx.doi.org/10.1016/j.jfoodeng.2009.01.014>
- Ramona, Mathieu, Richard, Guilhem, & David, Barak. (2012). Multiclass feature selection with kernel gram-matrix-based criteria. *Neural Networks and Learning Systems, IEEE Transactions on*, 23(10), 1611-1623.
- Sankaran, Sindhuja, Ehsani, Reza, & Etxeberria, Edgardo. (2010). Mid-infrared spectroscopy for detection of Huanglongbing (greening) in citrus leaves. *Talanta*, 83(2), 574-581. doi: <http://dx.doi.org/10.1016/j.talanta.2010.10.008>
- Sankaran, Sindhuja, Mishra, Ashish, Maja, Joe Mari, & Ehsani, Reza. (2011). Visible-near infrared spectroscopy for detection of Huanglongbing in citrus orchards. *Computers and Electronics in Agriculture*, 77(2), 127-134. doi: 10.1016/j.compag.2011.03.004
- Schubert, Tim, Sutton, Bruce, & Jeyaprakash, Ayyamperumal. (2010). Citrus Black Spot (*Guignardia citricarpa*) discovered in Florida. <http://syndication.freshfromflorida.com/content/download/9770/134888/guignardia-citricarpa.pdf>